# Digital-twin imaging based on descattering Gaussian splatting

SUGURU SHIMOMURA,* KAZUKI YAMANOUCHI, AND JUN TANIDA

*Graduate School of Information Science and Technology, The University of Osaka, 1-5 Yamadaoka, Suita, Osaka, Japan*

*s-shimomura@ist.osaka-u.ac.jp*

**Abstract:** Three-dimensional imaging through scattering media is important in medical science and astronomy. We propose a digital-twin imaging method based on Gaussian splatting to observe an object behind a scattering medium. A digital twin model built through data assimilation, emulates the behavior of objects and environmental changes in a virtual space. By constructing a digital twin using point clouds composed of Gaussians and simulating the scattering process through the convolution of a point spread function, three-dimensional objects behind a scattering medium can be reproduced as a digital twin. In this study, a high-contrast digital twin reproducing a three-dimensional object was successfully constructed from degraded images, assuming that data were acquired from wavefronts disturbed by a scattering medium. This technique reproduces objects by integrating data processing with image measurements.

## 1. Introduction

Optical imaging is a fundamental technology for observing objects and is widely applied in various fields including medical science and astronomy. High-resolution or high-contrast imaging enables the observation of deep tissue conditions *in vivo*, providing an understanding of biological mechanisms. In astronomy, observing distant objects furthers our understanding of the universe. However, scattering media distort optical wavefronts, making it difficult to observe the target objects accurately. Obtaining information about objects from optical signals scattered by the environment remains challenging, and several data processing-based methods have been proposed.

Computational imaging is a promising approach for extracting object information from scattered signals by combining optical and computational processing [1–3]. For example, Richardson–Lucy and Wiener deconvolutions are well-known methods for removing scattering effects from degraded images [4]. Modeling a scattering medium allows for the reproduction of light propagation and the recovery of object structures [5, 6]. Digital holography techniques reconstruct object images from the interference patterns of the speckles and reference beams [7–9]. In addition, speckle correlation and phase retrieval algorithms offer noninvasive imaging for observing objects behind a scattering medium [10–13]. Another approach involves estimating the transmission matrix that characterizes light propagation [14]. The transmission matrix can be estimated by measuring the optical responses of the object, and the object can be reconstructed using the matrix inverse function [15, 16]. Machine learning enables the modeling of scattering processes and reconstruction of object images from speckle patterns [17–19]. Computational imaging can provide high-contrast object images from scattered signals by employing various retrieval algorithms. In these methods, it is important to obtain the light-scattering response from a limited spatial region in advance. The contrast and spatial resolution of the reconstructed image depend on the amount of captured data, and long measurement times are required to extend the field of view behind the scattering medium. In conventional methods, object reconstruction is performed under the assumption that the scattering medium remains time invariant. However, biological and atmospheric turbulence changes dynamically, making it difficult to reconstruct images based on previously obtained data. In addition, reconstructing three-dimensional (3D) objects requires multiple measurements depending on the cross-sectional view of the recon-

structed object. Consequently, efficient reconstruction of 3D objects from images degraded by scattering remains a significant challenge. These issues can be addressed by simultaneously optimizing the measurement and reconstruction by integrating optical and computational processing.

A digital twin constructed through data assimilation is a promising technology for integrating data acquisition and processing [20]. Through simulation using digital-twin dynamics, the environmental and object changes can be emulated in cyberspace. The emulation results are analyzed and fed back into the data acquisition method in the physical space. The digital twin is updated by using the acquired data and utilized for the emulation again. By iterative update, the emulation accurately reproduces the changes in the physical system. The use of a digital twin not only reproduces, but also predicts object behavior through iterative emulation and analysis, facilitating optimization and decision-making for efficient data acquisition. By integrating a digital twin into computational imaging, complex light scattering can be modeled, analyzed, and used to efficiently reproduce objects behind the scattering media.

This paper presents a digital-twin imaging method for reproducing 3D objects behind the scattering media. In the proposed method, a digital twin representing the object behind the scattering medium is constructed using captured images that are degraded by scattering. By emulating the scattering process in cyberspace and iteratively updating the digital twin, the 3D structure of the object can be reproduced. Construction of a digital twin requires modeling the target object. We employed a method that models an object as a collection of points, allowing for flexible adaptation without a predefined spatial resolution. The optical response of an object can be described as the sum of the signals at each point. Thus, an image of the target object can be obtained if the individual optical responses are accurately reproduced in cyberspace. To represent the digital twin as point clouds, we employed Gaussian splatting (GS), which represents a 3D space using Gaussians [21]. In GS, 3D objects are flexibly represented by optimizing the parameters of each Gaussian based on images captured from multiple viewpoints. Previous studies demonstrated 3D imaging of the human body based on coherent tomography using GS [22, 23]. Furthermore, combining neural fields with GS enables the creation of realistic 3D spaces without motion blurring [24, 25]. In the proposed method, the digital twin is constructed and iteratively updated based on a GS algorithm that incorporates the scattering process. To validate the proposed method, we evaluated the structure of a digital twin constructed from blurred images captured from multiple viewpoints.

## 2. Digital twin constructed and updated by descattering Gaussian splatting

For realizing the digital-twin imaging, it is important to construct and update a digital twin by modeling the target object and phenomena in cyberspace and by using the measurement data. To reproduce an object behind a scattering medium from the degraded images, each Gaussian' s parameters are optimized such that their rendered images, which degraded by a virtually simulated scattering process, correspond to the actual captured images. Hereafter, we refer to GS incorporating the scattering process as descattering Gaussian splatting (DGS). Figure 1 shows the DGS process. Initially, the target object behind the scattering medium is captured from multiple viewpoints. The initial point cloud are distributed in the 3D space, and the parameters of each Gaussian are initialized. These points are then converted into Gaussians using the following equation:

$$G(x) = e^{-\frac{1}{2}(x-\mu_i)^T \Sigma_i (x-\mu_i)}, \tag{1}$$

where $\boldsymbol{x}$ are the spatial coordinates, and $\mu_i$ is the center position of the $i$-th point. $\Sigma$ is the 3D covariance matrix that represents the shape of the Gaussian. Individual Gaussians have parameters $\alpha$ and spherical harmonic coefficient $c$, which represent their opacity and color, respectively. The Gaussians are then projected onto a 2D image by rendering. During the

projection, the 3D covariance matrix $\Sigma$ [26] is converted into a 2D covariance for rendering. After converting the parameters of the individual Gaussians to 2D, the images are rendered by a differentiable tile rasterizer using the positions and poses estimated from the captured images. Each pixel value $I_{\text{pix}}$ in the rendered image $I_{GS}$ is formulated as an alpha blending of $N$ ordered points that overlap the pixel:

$$I_{\text{pix}} = \Sigma_i^N c_i \alpha_i^{2D} \prod_j^{i-1} (1 - \alpha_j^{2D}), \tag{2}$$

where $\alpha_i^{2D}$ is the opacity of the $i$-th Gaussian weighted by the 2D Gaussian covariance $\Sigma^{2D}$ to $\alpha_i$. To construct a digital twin for modeling the target object behind a scattering medium using Gaussians, the scattering and optimization processes must be integrated. In the proposed method, we introduce a scattering process by convolution with a point spread function (PSF) which represents the light propagation through the scattering medium. In the proposed method, the rendered images $I_{GS}$ are virtually degraded into $I_{deg}$ by convolving them with a point spread function (PSF) representing light propagation:

$$I_{deg} = \text{PSF} \otimes I_{GS}, \tag{3}$$

where $\otimes$ denotes a convolution operation. The use of PSF allows the simulation of the scattering process in cyberspace, thereby enabling the construction of a digital twin of a 3D object behind the scattering medium. The loss function $L$ was computed using the mean absolute error (MAE) and structural similarity index measure (SSIM) between the rendered images after convolution and the captured images. Each Gaussian' s parameters are updated through backward processing of the loss function via deconvolution of virtually degraded images. In conventional GS, the digital twin is constructed from degraded images, and the reconstructed object remains blurred. In contrast, the proposed DGS constructs the digital twin of the target object using information prior to light degradation, by explicitly modeling the scattering process. As a result, the object behind the scattering medium can be reconstructed accurately. In adaptive density control, Gaussians are split, cloned, or removed based on the gradient of the loss function $L$. Through optimization process, the digital twin, which consists of Gaussians, is continuously updated using both virtual and actual images. Finally, the emulation results in cyberspace represent the actual them in real space, and therefore, the digital twin can reproduce the object behind the scattering medium.

## 3. 3D object reproduction by digital-twin imaging based on DGS

To evaluate the performance of the proposed method, we reproduced a 3D object as a digital twin from blurred images.

### *3.1. Experimental setup*

To construct a digital twin using DGS with a descattering process, it is necessary to capture the target object from multiple viewpoints. Figure 2 shows the experimental setup to acquire images from various angles. The target object was placed at the center of a table, and a rail was positioned along its side. The target object was imaged using a CMOS camera (Sony $\alpha$7III). The camera moved along the rail, covering a length of 420 mm, corresponding to a 36.6 $\circ$ field of view. The distance between the camera and the target object was set to 280 mm to ensure that the entire object and its surface could be observed in the captured images. The focal length of the lens was set to 105 mm, and the imaging area was $575 \times 385$ mm$^2$ at the center of the rail.

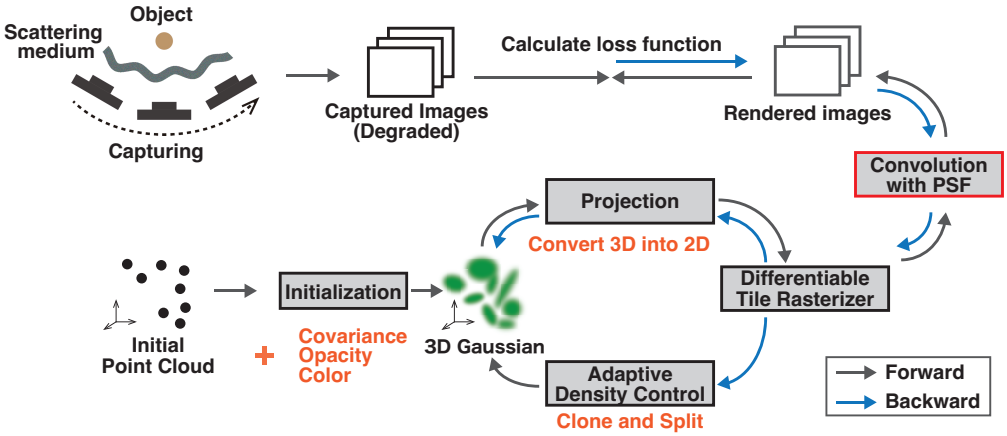


Fig. 1. DGS to construct a digital twin of the target object using images degraded by a scattering medium.

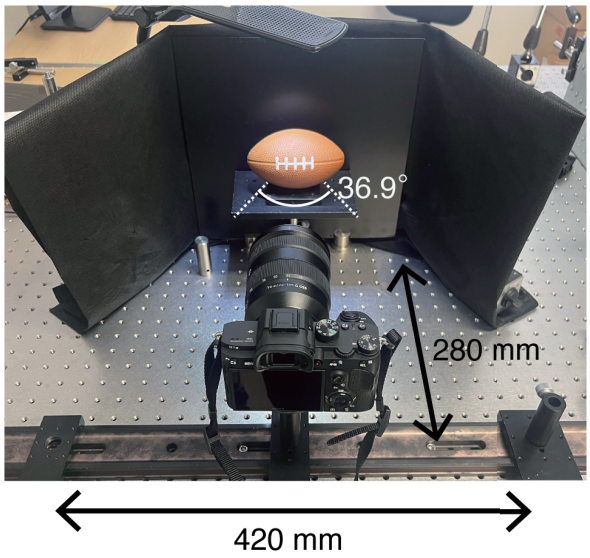


Fig. 2. Experimental setup for imaging the target object from various viewpoints.

### *3.2. Digital twin with three-dimensional structure constructed by DGS*

To assess the performance of the proposed method, digital twins were constructed from blurred images. A rugby ball with an uneven surface was used as the target object [Fig. 3 (a)]. By using structure from motion (SfM), which estimates camera parameters, including position and orientation, initial points clouds are generated [27,28]. To validate the proposed method, images degraded by the scattering medium were virtually generated by convolving the captured images using a PSF. Assuming a scattering process, the PSF was modeled as a 2D Gaussian distribution with a standard deviation of five pixels as shown in Fig. 3 (b). To investigate whether DGS can reproduce the scattering process and reconstruct a three-dimensional object from blurred images, we compared and evaluated the surface details of the digital twins constructed using the proposed DGS with that constructed using conventional GS. Figures 3 (c) and (d) show the

digital twins constructed using the conventional GS and the proposed DGS, respectively. A total of 76 images were utilized as inputs to SfM within each framework. The rendered views of each digital twin and the captured images from various angles are provided in Supplementary Material Visualization 1. The surface of the ball constructed using the conventional GS was blurred [Fig. 3 (c)]. By contrast, the topography of the digital twin constructed using DGS was clearly reproduced [Fig. 3(d)]. Figures 3 (e) and (f) show pixel intensity profiles along the blue lines in Figures 3 (c) and (d), respectively. The pixel values of individual profiles are normalized with respect to their respective maximum values. With the conventional GS, the regions representing the uneven surface of the ball were not reproduced, although the white lines were preserved. The proposed method successfully constructed the digital twin with an uneven surface that closely corresponded to the ground truth, as measured from the actual images of the rugby ball. The mean squared error (MSE) between the pixel values of the ground truth and those of the conventional GS was 9.7. In contrast, the MSE of the proposed DGS was 3.6. These results demonstrate that integrating the scattering and construction processes allows the digital twin to retain fine surface details, even when generated from blurred images. To evaluate 3D structural reproducibility, the widths of the red lines with arrows were measured from virtually generated images captured from multiple angles. Figure 3 (g) shows the measured linewidths from different viewpoints. The widths of the digital twin constructed using the proposed method closely matched those obtained from the actual images. The concordance ratio between the widths of the captured and rendered images was 0.26 for DGS, compared with 0.04 for conventional GS. These results confirm that the proposed method effectively reproduces 3D objects with high fidelity. In the case of a PSF with a standard deviation of more than twenty pixels, the digital twin could not be constructed using DGS. This is because the degradation effect caused the characteristic points in the captured images to be lost, preventing the SfM from generating initial points. To construct a digital twin under strong degradation conditions, the initial points must be generated without characteristic points.

### *3.3. Position estimation of a light-emitting diode array using DGS*

Next, we evaluated the accuracy of the digital twin constructed via DGS by estimating the position of a light-emitting diode (LED) array from degraded images by scattering. As a target object, We employed a LED array with three LEDs (LED-1, LED-2, and LED-3) arranged in a three-dimensional space [Fig. 4 (a)]. A diffuser (Optical Solutions, LSD 1° ) was placed in front of the camera [Fig. 4 (b)]. To emulate the scattering process in the DGS, captured images of LED-2 behind the diffuser at individual viewpoints were used as PSFs [Fig. 4 (c)]. The obtained PSFs was modeled as a 2D Gaussian distribution, and their standard deviations were estimated to between 28 and 36 pixels. The initial point clouds were generated randomly in the cyberspace, and the camera parameters and the center of target object for the projection process were estimated by Blender [29]. Figures 4(d) and (e) show the images captured with and without the diffuser, respectively. The diffuser scattered light from the LED array and made the positions of the LEDs indistinct in the captured images. Using the degraded images and the DGS, a digital twin was constructed. A rendered image of the digital twin is shown in Fig. 4 (f), The digital twin was constructed from 61 images captured from various viewpoints. Multiple views of the PSFs, captured images with and without the diffuser, and rendered images of the digital twin are provided in Supplementary Material Visualization 2. The constructed digital twin reproduces the shape of the LED array. The center positions of the individual LEDs were estimated by obtaining the centroid of the Gaussian clouds. To assess the accuracy of the position estimation, we determined the depth of each LED using a triangulation method. The depth values were iteratively calculated from pairs of the 61 captured images, and the average depth for each LED was used as its ground truth. While the depths of the LED-1, LED-2 and LED-3 were 437.7, 416.7, and 393.6 mm, the centroid depths of the Gaussian clouds were 436.7, 415.3,

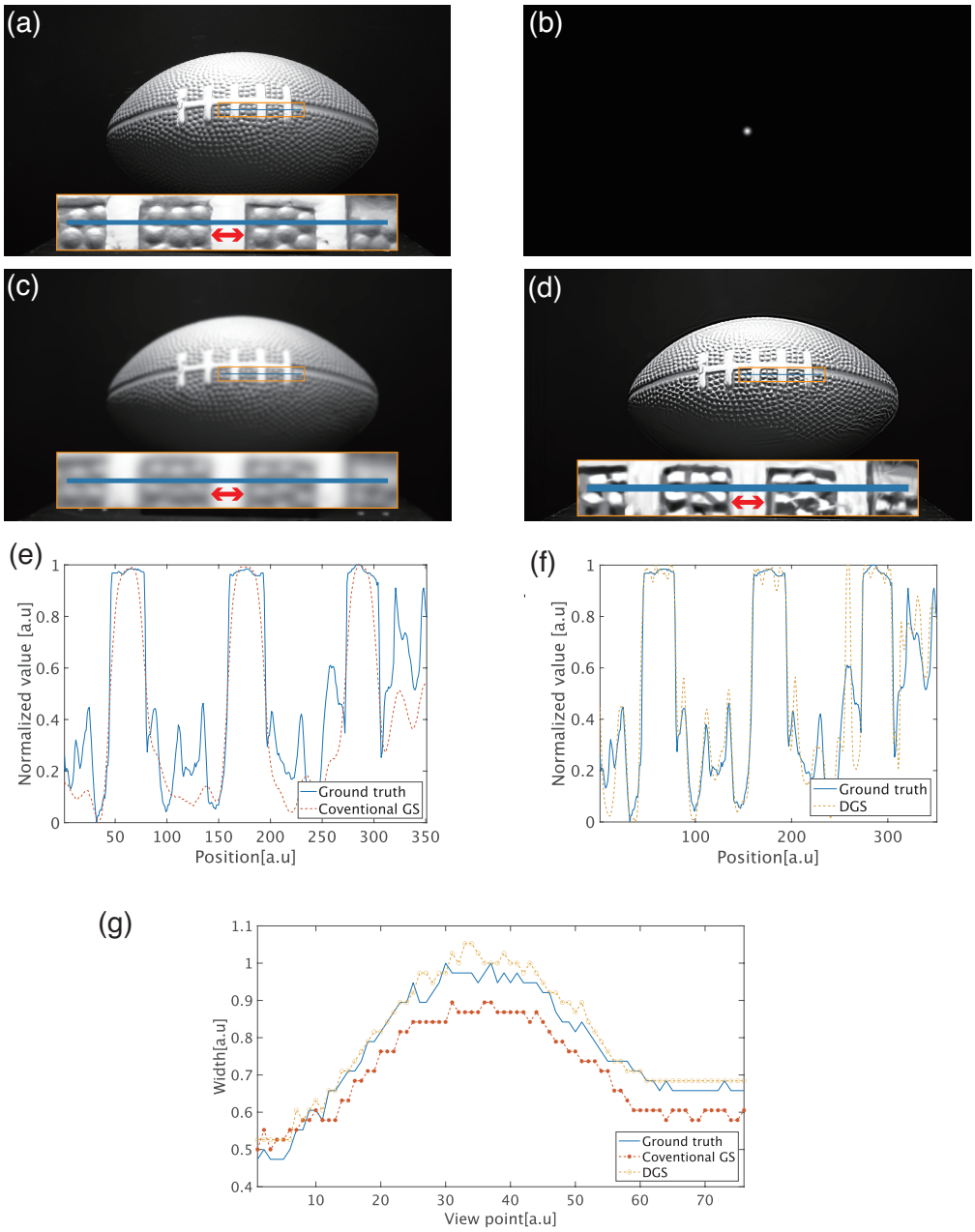


Fig. 3. (a) An image captured from a single viewpoint. (d) A point spread function for emulating the scattering process. Rendered images of the digital twins using (c) conventional GS and (d) proposed DGS. The bottom sections of (c) and (d) show enlarged views of the areas highlighted by orange squares. (e, f) Pixel value profiles along the blue lines shown in (c) and (d), respectively. (g) Linewidths along the red lines with arrows in (c) and (d) from various viewpoints.

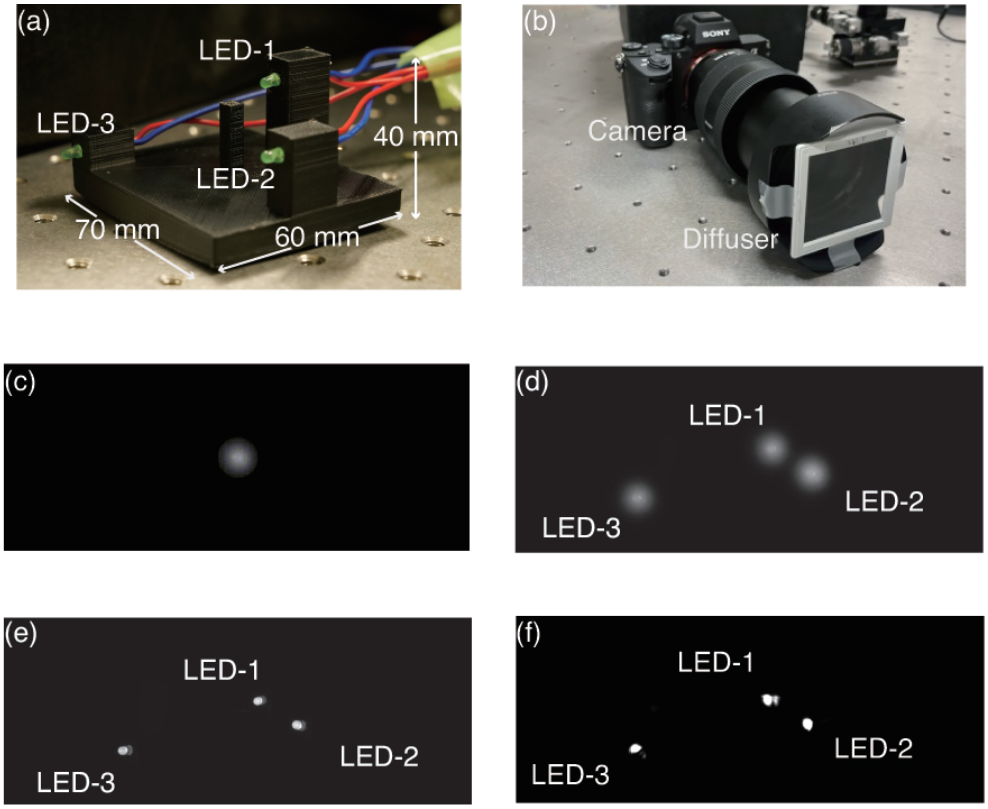


Fig. 4. (a) LED array used for the target object. (b) Optical setup for capturing the LED array behind a diffuser. (c) Captured image of LED-2 with a diffuser, used as a PSF. Images captured (d) with a diffuser and (e) without a diffuser. (f) Rendered images of the digital twin constructed using DGS.

and 391.2, respectively. The average errors was 1.1 mm. These values indicate that the depth positions of the Gaussians are consistent with those obtained from the triangulation method. These results demonstrate that the digital twin constructed using DGS accurately reproduces the spatial distribution of the LED array.

## 4. Discussion

The use of a digital twin enables not only the reconstruction of a three-dimensional structure but also the representation of the object's properties based on the modeling. For example, detailed modeling of light propagation in scattering media reveals both the optical properties of the medium and the target object [15]. Furthermore, simulating beam propagation through an object represented as point clouds allows for the estimation of the refractive index distribution [30]. Depending on the modeling, multiple parameters that cannot be determined through a single type of measurement can be introduced to reveal the object's characteristics. The feedback from the constructed model can be used to optimize measurement conditions, improving both the accuracy of the digital twin and the efficiency of the measurements. For example, the back

side of an object, where no direct measurement data are available, can be estimated using a digital twin. This estimation can then provide feedback for subsequent measurements. The loss function also facilitates the refinement of actual camera parameters, such as position and orientation. Captured images, informed by feedback from the digital twin, are effectively used to optimize the parameters of the Gaussians representing the object. The loss function is applied iteratively to refine the camera parameters. This iterative process of optimizing the measurement conditions enables efficient acquisition of 3D object information while reducing the number of required images. Moreover, the feedback obtained from the digital twin can also be used to switch the measurement methods. Depending on the type of information desired, the measurement approach can be selected from various methods such as optical imaging and spectroscopy, allowing efficient acquisition of multimodal information about the object. Digital twin imaging is expected to be applied not only to optical measurements but also to various other measurement techniques by utilizing the obtained feedback.

In this paper, we propose a digital-twin imaging method to model and reproduce the target object using DGS. The convolution of PSF integrated into GS reproduces the scattering process during image capture. The experimental results demonstrated that the topography of the digital twin constructed from the blurred images corresponded to that of the real object. Our findings suggest that digital-twin imaging can serve as an effective approach for observing objects behind scattering media.

**Funding.** JSPS KAKENHI (Grant Number 20H05890, 25K21339).

**Disclosures.** The authors declare no conflicts of interest.

**Data availability.** Data underlying the results presented in this paper are not publicly available at this time but may be obtained from the authors upon reasonable request.

## References

1. A. P. Mosk, A. Lagendijk, G. Lerosey, and M. Fink, "Controlling waves in space and time for imaging and focusing in complex media," Nat. photonics **6**, 283–292 (2012).
2. S. Yoon, M. Kim, M. Jang, *et al.*, "Deep optical imaging within complex scattering media," (2020).
3. S. Gigan, O. Katz, H. B. De Aguiar, *et al.*, "Roadmap on wavefront shaping and deep imaging in complex media," (2022).
4. A. Levin, Y. Weiss, F. Durand, and W. T. Freeman, "Understanding and evaluating blind deconvolution algorithms," 2009 IEEE Conf. on Comput. Vis. Pattern Recognit. pp. 1964–1971 (2009).
5. S. Kang, Y. Kwon, H. Lee, *et al.*, "Tracing multiple scattering trajectories for deep optical imaging in scattering media," Nat. Commun. **14**, 1–12 (2023).
6. A. Thendiyammal, G. Osnabrugge, T. Knop, and I. M. Vellekoop, "Model-based wavefront shaping microscopy," Opt. letters **45**, 5101–5104 (2020).
7. A. K. Singh, D. N. Naik, G. Pedrini, *et al.*, "Looking through a diffuser and around an opaque surface : A holographic approach," Opt. Express **22**, 7694–7701 (2014).
8. A. S. Somkuwar, B. Das, R. Vinu, *et al.*, "Holographic imaging through a scattering layer using speckle interferometry," JOSA A **34**, 1392–1399 (2017).
9. J. Bertolotti, E. G. Van Putten, C. Blum, *et al.*, "Non-invasive imaging through opaque scattering layers," Nature **491**, 232–234 (2012).
10. O. Katz, P. Heidmann, M. Fink, and S. Gigan, "Non-invasive single-shot imaging through scattering layers and around corners via speckle correlations," Nat. Photonics **8**, 784–790 (2014).
11. Y. Okamoto, R. Horisaki, and J. Tanida, "Noninvasive three-dimensional imaging through scattering media by three-dimensional speckle correlation," Opt. Lett. **44**, 2526 (2019).
12. Z. Wang, X. Jin, and Q. Dai, "Non-invasive imaging through strongly scattering media based on speckle pattern estimation and deconvolution," Sci. Reports **8**, 1–11 (2018).
13. T. Yeminy and O. Katz, "Guidestar-free image-guided wavefront shaping," Sci. advances **7**, eabf5364 (2021).
14. S. M. Popoff, G. Lerosey, M. Fink, *et al.*, "Controlling light through optical disordered media: transmission matrix approach," New J. Phys. **13**, 123021 (2011).
15. S. M. Popoff, G. Lerosey, R. Carminati, *et al.*, "Measuring the transmission matrix in optics: An approach to the study and control of light propagation in disordered media," Phys. Rev. Lett. **104**, 1–4 (2010).
16. A. Boniface, J. Dong, and S. Gigan, "Non-invasive focusing and imaging in scattering media with a fluorescence-based transmission matrix," Nat. communications **11**, 6154 (2020).

17. R. Horisaki, R. Takagi, and J. Tanida, "Learning-based imaging through scattering media," Opt. express **24**, 13738–13743 (2016).
18. Y. Nishizaki, M. Valdivia, R. Horisaki, *et al.*, "Deep learning wavefront sensing," Opt. express **27**, 240–251 (2019).
19. H. Liu, F. Wang, Y. Jin, *et al.*, "Learning-based real-time imaging through dynamic scattering media," Light. Sci. Appl. **13** (2024).
20. F. Tao, B. Xiao, Q. Qi, *et al.*, "Digital twin modeling," J. Manuf. Syst. **64**, 372–389 (2022).
21. B. Kerbl, G. Kopanas, T. Leimkuehler, and G. Drettakis, "3D Gaussian Splatting for Real-Time Radiance Field Rendering," (2023).
22. Y. Li, X. Fu, S. Zhao, *et al.*, "Sparse-view CT Reconstruction with 3D Gaussian Volumetric Representation," (2023).
23. Y. Cai, Y. Liang, J. Wang, *et al.*, "Radiative Gaussian Splatting for Efficient X-ray Novel View Synthesis," (2024).
24. B. Lee, H. Lee, X. Sun, *et al.*, "Deblurring 3D Gaussian Splatting," (2024).
25. O. Seiskari, J. Ylilammi, V. Kaatrasalo, *et al.*, "Gaussian Splatting on the Move: Blur and Rolling Shutter Compensation for Natural Camera Motion," (2024).
26. M. Zwicker, H. Pfister, J. Van Baar, and M. Gross, "Ewa volume splatting," in *Proceedings Visualization, 2001. VIS'01.*, (IEEE, 2001), pp. 29–538.
27. J. L. Schonberger and J.-M. Frahm, "Structure-from-motion revisited," in *Proceedings of the IEEE conference on computer vision and pattern recognition,* (2016), pp. 4104–4113.
28. N. Snavely, S. M. Seitz, and R. Szeliski, "Photo Tourism : Exploring Photo Collections in 3D," in *ACM siggraph 2006 papers,* (2006), pp. 835–846.
29. J. van Gumster, *Blender For Dummies* (For Dummies, 2015), 3rd ed.
30. H. Wang, W. Tahir, J. Zhu, and L. Tian, "Large-scale holographic particle 3d imaging with the beam propagation model," Opt. express **29**, 29 (2021).